Unraveling the couplings of a Drell-Yan produced Z' with heavy-flavor tagging

Wei-Shu Hou,[1,2] Masaya Kohda,[1] and Tanmoy Modak[1]
[1]Department of Physics, National Taiwan University, Taipei 10617, Taiwan
[2]ARC CoEPP at the Terascale, School of Physics, University of Melbourne, Victoria 3010, Australia

(Received 15 January 2018; published 3 July 2018)

Despite the current absence of new-physics signals at the LHC, a Z' boson with $m_{Z'} \sim 100$ GeV could still emerge via Drell-Yan (DY) production, $q\bar{q} \to Z' \to \mu^+\mu^-$, in the next few years. To unravel the nature of the Z' coupling, we utilize the c- and b-tagging algorithms developed by ATLAS and CMS to investigate $cg \to cZ'$ at the 14 TeV LHC. While light-jet contamination can be eliminated, mistagged b jets cannot be rejected in any of the tagging schemes we adopt. On the other hand, for nonzero bbZ' coupling, far superior b tagging could discover the $bg \to bZ'$ process, where again light-jet mistagging can be ruled out, but mistagged c jets cannot yet be excluded. Provided that DY production is discovered soon enough, we find that a simultaneous search for $cg \to cZ'$ and $bg \to bZ'$ can conclusively discern the nature of the Z' couplings involved.

DOI: 10.1103/PhysRevD.98.015002

I. INTRODUCTION

A Z' boson with a mass of a few hundred GeV could still emerge via the Drell-Yan (DY) process, $q\bar{q} \to Z' \to \mu^+\mu^-$, for qqZ' couplings that are weaker than analogous Standard Model (SM) couplings. Recent searches [1,2] set stringent bounds on the couplings of such a Z' boson to u, d, and s quarks, but the limits are much weaker for c or b quarks; hence, discovery is possible within the next few years. One such scenario [3] involves a Z' that couples to c quarks, leading to DY production $c\bar{c} \to Z' \to \mu^+\mu^-$ at the LHC. The $cg \to cZ' \to c\mu^+\mu^-$ process then offers a unique probe of the flavor structure of the Z' coupling if the c-jet flavor can be identified. Recent developments at ATLAS and CMS in c-tagging [4–6] algorithms and the excellent performance of b tagging [5,7,8] offer such an opportunity. In this paper we discuss how these heavy-flavor taggers can probe the couplings of a Z' after its discovery through the DY process.

We illustrate by using the scenario of Ref. [3], where a Z' couples relatively weakly to charm quarks and predominantly to muons. The DY process $pp \to Z' + X \to \mu^+\mu^- + X$ (with X being an inclusive activity) could emerge in the next few years, and a ccZ' coupling would imply the $cg \to cZ'$ process. We apply the c-tagging algorithms to investigate the discovery potential of $pp \to cZ' + X \to c\mu^+\mu^- + X$ (denoted as the cZ' process, with the conjugate process implied) at the $\sqrt{s} = 14$ TeV LHC.

The c-tagging algorithms of ATLAS [4,5] and CMS [6] discriminate c jets from light jets (jets originating from u, d, s, and gluons) at the expense of c-tagging efficiency, while the misidentification (or mistag) rate of b jets as c jets is relatively sizable. If the Z' couples to light $q = u$, d, s quarks, a potential cZ' signal may arise from mistagging (denoted as a fake cZ'). As qqZ' coupling is constrained by searches for heavy resonances in the DY process [1], our analysis shows that in certain c-tagging schemes one can completely rule out the possibility of fake cZ''s from light jets. But these tagging schemes fail to rule out the possibility of fake cZ''s from mistagged b jets.

In case the Z' couples instead to b quarks (bbZ' coupling), $pp \to bZ' + X \to b\mu^+\mu^- + X$ (the bZ' process) would emerge after the discovery in the DY process. This process could be observed by the well-developed b-tagging algorithms [5,7,8], which provide excellent discrimination against light and c jets while maintaining high b-tagging efficiency. We find that the current limit on ccZ' coupling allows for fake bZ' discovery at the LHC due to the mistagging of c jets as b jets. However, this fake bZ' process at the LHC could be ruled out if $\sim$250 fb^{-1} data is collected. We find that, if a Z' is discovered via the DY process in the next few years, by combining the cZ' and bZ' signatures together with current limits from heavy resonance searches one can conclusively infer the nature of Z' couplings.

We finally consider a case where both bbZ' and ccZ' couplings are nonzero and study DY, cZ', and bZ' processes for a representative Z' mass. We find that the coupling structure of such a scenario can also be disentangled if it is combined with the current limit from heavy resonance searches in the DY process.

The paper is organized as follows. In Sec. II, we analyze the discovery potential of the DY process due to qqZ'

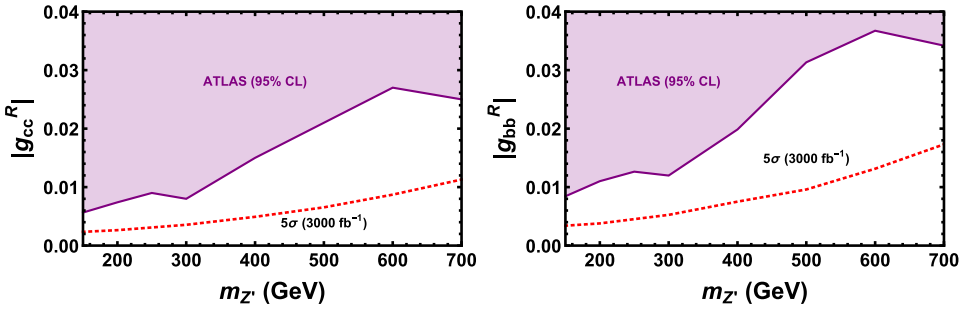

FIG. 1. The 5σ discovery reach of the DY process $pp \to Z' + X \to \mu^+\mu^- + X$ at the 14 TeV LHC with 3000 fb^{-1} data, initiated by ccZ' (left) and bbZ' (right) couplings. The purple shaded regions are the 95% CL upper limits extracted from Ref. [1].

couplings. In Sec. III, we apply different c-tagging algorithms for the discovery potential of the cZ' process and discuss fake sources. Section IV is dedicated to the bZ' process and disentangling the Z' coupling structure by combining it with the results of Sec. III. The scenario with both ccZ' and bbZ' couplings is analyzed in Sec. V, and we summarize in Sec. VI. The analysis for the DY process is detailed in Appendix A, while normalized kinematic distributions for the signal and backgrounds of the cZ' process are provided in Appendix B.

II. THE DRELL-YAN PROCESS

We take the following effective couplings:

$$\mathcal{L} \supset -g'(\bar{\mu}\gamma_\alpha\mu + \bar{\nu}_{\mu L}\gamma_\alpha\nu_{\mu L} - \bar{\tau}\gamma_\alpha\tau - \bar{\nu}_{\tau L}\gamma_\alpha\nu_{\tau L})Z'^\alpha - \sum_{q=u,d,s}^{c,b} g_{qq}^R \bar{q}_R\gamma_\alpha q_R Z'^\alpha, \quad (1)$$

where g' is the coupling of Z' to the muon, tauon, and their neutrinos, and g_{qq}^R is the right-handed qqZ' coupling (induced by some underlying heavy particles [9]). The context is the effective model based on the gauged $L_\mu - L_\tau$ [10,11] symmetry, as discussed in Refs. [9,12]. For simplicity and to be more general, we set all flavor-violating couplings to zero and assume g_{qq}^R to be real. The coupling g' is taken to be much larger than the coupling g_{qq}^R; hence, the Z' couples more weakly to quarks, and its decay branching ratios can be approximated as

$$\mathcal{B}(Z' \to \mu^+\mu^-) \simeq \mathcal{B}(Z' \to \tau^+\tau^-) \simeq \mathcal{B}(Z' \to \nu\bar{\nu}) \simeq \frac{1}{3}. \quad (2)$$

The results in this paper can be scaled to any narrow Z' that couples to quarks and muons by the relation

$$|g_{qq}^R| \to |g_{qq}^R|\sqrt{3 \times \mathcal{B}(Z' \to \mu^+\mu^-)}. \quad (3)$$

Searches for heavy dilepton resonances by ATLAS [1] and CMS [2] set stringent bounds on $\sigma(pp \to Z' + X) \cdot \mathcal{B}(Z' \to \mu^+\mu^-)$, and hence on g_{qq}^R couplings. The ATLAS result is based on 36 fb^{-1} data, while the CMS result is for 13 fb^{-1}. We use the former [1] to extract 95% credibility level (CL) upper limits on g_{cc}^R and g_{bb}^R couplings, shown as the purple shaded regions in Fig. 1. In doing so, we calculate $\sigma(pp \to Z' + X)$, where the dominant contribution is from $q\bar{q} \to Z'$ with subdominant contributions $qg \to qZ'$ and $gg \to q\bar{q}Z'$ ($q = c$ or b), at leading order (LO) for fixed $m_{Z'}$ and g_{qq}^R using MadGraph5_aMC@NLO (referred to as MadGraph5_aMC from here on) [13]; we generate matrix elements (MEs) with up to two additional jets in the final state[1] with the parton distribution function (PDF) set NN23LO1 [14], followed by Pythia 6.4 [15] using the MLM scheme [16] for ME and parton shower (PS) matching and merging. Then, we rescale the estimated cross section by $|g_{qq}^R|^2$ and extract the upper limit on $|g_{qq}^R|$ for each $m_{Z'}$ from the ATLAS result assuming $\mathcal{B}(Z' \to \mu^+\mu^-) \simeq 1/3$. In Fig. 1, the 5σ discovery reach[2] is also given with 3000 fb^{-1} data for the High-Luminosity LHC (HL-LHC). If the Z' couples to u, d, or s quarks, the limits on g_{qq}^R would be much stronger due to a larger PDF, i.e., it probes a much smaller g_{uu}^R, g_{dd}^R, or g_{ss}^R coupling than that of g_{cc}^R and g_{bb}^R. The details of the cut-based analysis and background processes are given in Appendix A. For the sake of a decent S/B ratio, we restrict ourselves to $m_{Z'} \lesssim 700$ GeV.

In principle, the methodology in this paper can be applied to left-handed qqZ' couplings g_{qq}^L, although there is some subtlety; that is, the $SU(2)_L$ gauge symmetry relates couplings of the up- and down-type sector quarks nontrivially. For instance, a nonzero g_{cc}^L is generally accompanied by a nonzero g_{ss}^L and all possible down-type sector couplings, e.g., g_{dd}^L, g_{bb}^L, and g_{bs}^L, which are Cabibbo-Kobayashi-Maskawa-suppressed. Hence, one has to deal with multiple couplings simultaneously. This would complicate the analysis, and we defer it to a future study.

III. THE cZ' PROCESS

Having discussed the discovery potential of ccZ' coupling through the DY process, we turn to $pp \to cZ' + X \to c\mu^+\mu^- + X$, i.e., the cZ' process, which requires the

[1]We restrict ourselves to up to two additional jets in the final state due to computational limitation.

[2]Significance is defined by $S/\sqrt{B}$, where S and B denote the number of signal and background events, respectively.

TABLE I. ATLAS [5] and CMS [6] c-, b-, and light-jet tagging efficiencies ϵ_c, ϵ_b, and ϵ_{light} for different working points.

	c tagger	ϵ_c	ϵ_b	ϵ_{light}
ATLAS	*Conf1*	0.4	0.17	0.1
	Conf2	0.2	0.1	0.004
CMS	*ctagL*	0.9	0.45	0.99
	ctagM	0.39	0.26	0.19
	ctagT	0.2	0.24	0.02

tagging of a c jet. Thanks to recent developments in charm tagging by ATLAS [5] and CMS [6], it is now possible to study such a process, and many phenomenological studies and discussions can already be found [17–25].

A. Searching for cZ'

Let us briefly discuss the present c-tagging algorithms. ATLAS [5] gives a range for b- and light-jet rejections[3] for a fixed value of the c-tagging efficiency. These fixed c-tagging efficiencies are presented as curves (called "iso-efficiency curves") in the b- vs light-jet rejection plane. CMS [6] presents similar constant c-tagging efficiency curves in the b- and light-jet mistag efficiency plane. For ATLAS iso-efficiency curves, c-tagging schemes with high light-jet rejection have low b-jet rejection rates, and vice versa. The CMS curves show similar behavior.

The largest background for the cZ' process is Z/γ^*+ light jet. In order to reduce this background, we take two c-tagging working points (WPs) with low light-jet mistag rates (i.e., high light-jet rejection) from the ATLAS analysis, which we call configuration 1 (Conf1) and configuration 2 (Conf2), given in the first two rows of Table I. On the other hand, CMS gives three c-tagging WPs called c-tagger L, M, and T (abbreviated as ctagL, ctagM, and ctagT in this paper), which we give in the last three rows of Table I. For both ATLAS and CMS, WPs with higher b-jet rejection could be taken at the cost of lower light-jet rejection for a fixed c-tagging efficiency, but we do not consider such cases in this study. Note that these c-tagging schemes show mild dependence on the transverse momentum (p_T) and pseudorapidity (η) of the jet. For simplicity, we take them to be constant in this study.

To illustrate the discovery potential of the cZ' process, we choose the benchmark values for the mass and coupling

$$m_{Z'} = 150 \text{ GeV}, \qquad g^R_{cc} = 0.005,$$

setting all other g^R_{qq} couplings in Eq. (1) to zero.

The cZ' process suffers from several SM backgrounds. The dominant ones are $Z/\gamma^* +$ jet, $t\bar{t}$, and Wt, with smaller contributions from WW, WZ, ZZ, $t\bar{t}Z$, $t\bar{t}W$, and tWZ. There exist nonprompt and fake backgrounds such as $W +$ jets, QCD multijets, etc., which we do not consider, as these backgrounds are not properly modeled in simulations. Due to different tagging efficiencies and mistag rates, we separate Z/γ^*+ jet background into three different categories, i.e., $Z/\gamma^* + c$ jet, b jet, and light jet, respectively.

Signal and background events are generated at LO in the pp collision with $\sqrt{s} = 14$ TeV via the Monte Carlo event generator MADGRAPH5_AMC@NLO with the PDF set NN23LO1, interfaced to PYTHIA 6.4 for showering and hadronization. The event samples are finally fed into the fast detector simulator DELPHES 3.4.0 [26] for inclusion of (CMS-based) detector effects. For ME and PS matching and merging, we follow the MLM matching scheme. To take higher-order corrections into account, the LO cross section of $Z+$ light jet is normalized by a correction factor of 1.83 [27] up to NNLO. For simplicity, we assume that the correction factors for the $Z + c$-jet and $Z + b$-jet backgrounds are the same as that for the $Z+$ light jet. The LO $t\bar{t}$ and Wt cross sections are normalized to the NNLO + NNLL ones by factors 1.84 [28] and 1.35 [29], respectively. Furthermore, the LO cross sections of WW, WZ, and ZZ backgrounds are normalized to the NNLO QCD ones by factors of 1.98 [30], 2.07 [31], and 1.74 [32], respectively. The NLO K factors for the $t\bar{t}Z$ and $t\bar{t}W^-$ ($t\bar{t}W^+$) backgrounds are assumed to be 1.56 [33] and 1.35 (1.27) [34]. We do not include K factors for the signal and the tWZ background.

We follow Ref. [25] closely in our analysis for both signal and background. We select events with two oppositely charged muons and at least one jet. Normalized event distributions can be found in Appendix B for transverse momenta of the two muons and leading c jet, and the invariant mass of a $\mu^+\mu^-$ pair. We require the leading and subleading muons to have $p_T^{\mu_1} > 50$ GeV, $p_T^{\mu_2} > 40$ GeV, respectively. The transverse momenta of the leading jet in an event should be $p_T^j > 45$ GeV. The minimum separation between two muons ($\Delta R_{\mu\mu}$) and the separation between any muon and the leading jet ($\Delta R_{\mu j}$) are required to be > 0.4. The maximum pseudorapidity ($|\eta|$) of both muons and the leading jet in an event are required to be < 2.5. The jets are reconstructed using the anti-k_T algorithm with radius parameter $R = 0.5$. To reduce contributions from $t\bar{t}$ and Wt backgrounds, events with missing transverse energy (E_T^{miss}) > 40 GeV are rejected. Finally, we impose an invariant-mass cut $|m_{\mu\mu} - m_{Z'}| < 15$ GeV on the two oppositely charged muons in an event. If an event contains more than one $m_{\mu\mu}$ combination, the combination closest to $m_{Z'}$ is selected. The impact of the selection cuts on the signal and backgrounds are given in Table II (based on ATLAS c tagging) and Table III (based on CMS c tagging).

The ATLAS Conf1 and Conf2 schemes may discover the cZ' process with 930 and 1090 fb^{-1} integrated luminosities, respectively. The dominant background contribution for Conf1 is from Z/γ^*+ light jet, while $Z/\gamma^* + c$ jet

[3]The mistag rate is defined as the complement of the rejection rate.

TABLE II. Signal and background cross sections (in fb) after selection cuts for a 150 GeV Z' (with $g^R_{cc} = 0.005$) produced via $pp \to cZ' + X \to c\mu^+\mu^- + X$ at the 14 TeV LHC with ATLAS c-tagging schemes, where the last column gives the total background (Total Bkg.), with V denoting either a W or Z boson.

c tagger WP (ATLAS)	Signal	$Z/\gamma^* + c$ jet	$Z/\gamma^* + b$ jet	Z/γ^*+ light jet	$t\bar{t}$	Wt	VV	$t\bar{t}V$	tWZ	Total Bkg.
Conf1	1.34	14.52	3.04	34.66	11.52	1.11	1.37	0.01	0.01	66.24
Conf2	0.67	7.26	1.79	1.39	6.77	0.65	1.61	0.01	0.001	19.48

TABLE III. Same as Table II, but for CMS c-tagging schemes.

c tagger WP (CMS)	Signal	$Z/\gamma^* + c$ jet	$Z/\gamma^* + b$ jet	Z/γ^*+ light jet	$t\bar{t}$	Wt	VV	$t\bar{t}V$	tWZ	Total Bkg.
ctagL	3.02	36.31	8.04	343.14	30.48	2.93	3.7	0.06	0.01	421.03
ctagM	1.31	14.16	4.64	65.85	17.61	1.69	2.1	0.02	0.001	106.08
ctagT	0.67	7.26	4.29	6.93	16.26	1.56	1.94	0.02	0.001	38.25

constitutes the second largest background. This is distinctly different for Conf2: $Z/\gamma^* + c$ jet and $t\bar{t}$ provide the dominant and second largest contributions. A larger c-tagging efficiency makes Conf1 superior to Conf2 for discovery. Similarly, ctagL, ctagM, and ctagT for CMS could discover the cZ' process with 1150, 1550, and 2120 fb^{-1} integrated luminosities. The ctagL requires roughly the same luminosity as ATLAS Conf2, although the c-tagging efficiencies and b- and light-jet mistag rates are different. The larger c-tagging efficiency of ctagL is balanced by higher mistag rates for light and b jets. The smaller c-tagging efficiencies make the cZ' process harder to discover for ctagM and ctagT.

Following the same selection cuts,[4] we extend our analysis for a Z' mass up to 700 GeV. The discovery reaches for ATLAS Conf1 (orange dotted), Conf2 (orange solid), CMS ctagL (blue dot-dashed), ctagM (blue dotted), and ctagT (blue solid) with 3000 fb^{-1} of data are given in Fig. 2.

B. FAKE cZ'

Signal for cZ' process could arise from light- and b-jet mistags, which we display in Fig. 3 for the cases of g^R_{uu} (left), g^R_{ss} (middle), and g^R_{bb} (right) couplings, for the LHC at $\sqrt{s} = 14$ TeV with 3000 fb^{-1} of data. The purple shaded regions correspond to 95% CL upper limits extracted from Ref. [1]. Let us take a closer look.

The fake cZ' signals depend on the upper limits on qqZ' coupling and the c-tagging schemes adopted. The extraction of upper limits involves the underlying DY process $q\bar{q} \to Z'$, which depends on the initial-state quark PDFs, and is also proportional to $|g^R_{qq}|^2$. On the other hand, fake cZ' signals can originate from $qg \to qZ'$ and its conjugate process. Although also proportional to $|g^R_{qq}|^2$, the cross sections are suppressed by the $2 \to 2$ nature compared to the DY process, and depend on gluon and quark PDFs. Due to high light-jet rejection rates, the two c-tagging schemes Conf2 and ctagT can fully eliminate fake cZ' from light jets. That is, the 5σ contours for them lie in the excluded regions for both g^R_{uu} and g^R_{ss} couplings in the Z' mass range studied, unlike Conf1, ctagL, and ctagM, which exclude only some $m_{Z'}$ regions.

None of these schemes, however, shows promise in reducing the number of fakes coming from b-jet misidentification, since all schemes have considerable b-jet mistag rates. This can be seen from the rightmost panel of Fig. 3. The high light-jet rejection and low c-tagging efficiency (to reduce the dominant Z/γ^*+ light-jet and $Z/\gamma^* + c$-jet backgrounds) mean that ctagT performs the worst. However, although having the same c-tagging efficiency and even lower light-jet rejection, the lower b-jet mistag

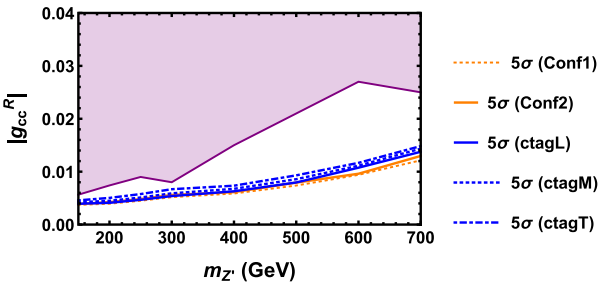

FIG. 2. The 5σ discovery reach of the $pp \to cZ' + X \to c\mu^+\mu^- + X$ process at 14 TeV with 3000 fb^{-1} of data. See text for details.

[4]Our study is for illustration, and we do not optimize the selection cuts for each $m_{Z'}$. However, we checked a possible impact of such a cut optimization. The largest impact would be obtained by narrowing the invariant mass window $|m_{\mu\mu} - m_{Z'}| <$ 15 GeV for a light Z': we found that, for $m_{Z'} = 150$ GeV, the 5 GeV window leads to an enhancement in the signal significance of ~30–34%, depending on the c-tagging scheme. We found that effects of changing the p_T cuts for the muons and leading c jet are minor, once we impose the $|m_{\mu\mu} - m_{Z'}|$ cut, which tends to select events with higher-p_T muons for a higher Z' mass.

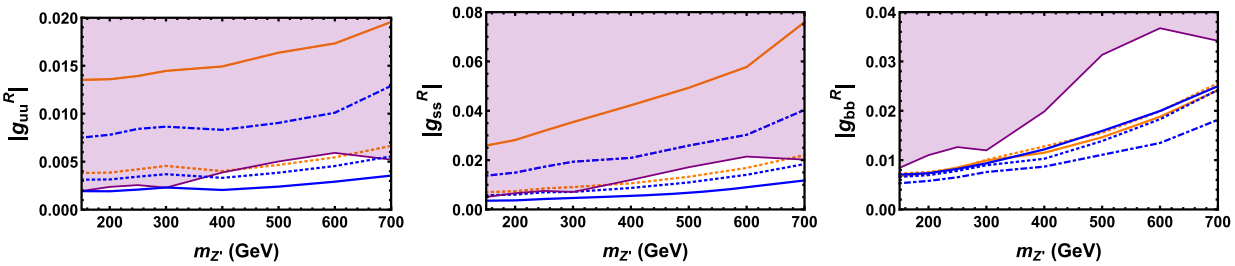

FIG. 3. The 5σ contours of fake cZ' arising from g_{qq}^R coupling at 14 TeV with 3000 fb^{-1} of data (color schemes are as in Fig. 2).

rate of Conf2 makes it perform better than ctagT. Our choice of high light-jet but moderate b-jet rejections allows the possibility of fake cZ' arising from bbZ' coupling. We thus turn to scrutinize this issue in the next section.

IV. THE bZ' PROCESS

A. Searching for bZ'

If the discovery of DY-produced Z' is due to bbZ' coupling, it implies that $bg \to bZ' \to b\mu^+\mu^-$ (and its conjugate) could also be discovered at the LHC. To illustrate the potential for $pp \to bZ' + X \to b\mu^+\mu^- + X$ at the LHC, we adopt a similar strategy as before, and take the following benchmarks for the mass and coupling:

$$m_{Z'} = 150 \text{ GeV}, \qquad g_{bb}^R = 0.005.$$

We follow the same cut-based analysis as in the previous section, except that the tag jet is now a b jet. We incorporate in DELPHES p_T- and η-dependent b-tagging efficiencies. The rejection factor of the light jets is taken as 137 [35]. For simplicity, we assume that the correction factors to the LO background cross sections generated by MADGRAPH5_AMC are the same as in the previous section, and we do not include a K factor for the signal. The signal and background cross sections after selection cuts are given in Table IV. The required luminosity to discover the 150 GeV Z' is 1180 fb^{-1}. Our analysis is further extended up to $m_{Z'} = 700$ GeV, as shown in the left panel of Fig. 4. For simplicity we choose the same selection cut as in the cZ' process to generate Fig. 4.

B. Fake bZ'

Mistagged light or c jets can also produce fake bZ' signals at the LHC, but the required g_{qq}^R couplings ($q = u, d, s$) to produce fake bZ' signals at 5σ with 3000 fb^{-1} are already disallowed by heavy resonance DY searches [1]. This attests to the excellent performance of b-tagging algorithms in reducing light-jet contributions. However, fake bZ' signals can still arise from mistagged c jets, except for two tiny mass windows around $m_{Z'} \sim 150$ and 300 GeV, as can be read from the right panel of Fig. 4 for the 5σ reach with 3000 fb^{-1}. We infer that, if no Z' is observed via DY with a $\sim$250 fb^{-1} data set, one can rule out the possibility of fake bZ' signals from the ccZ' coupling at LHC.

Even if a Z' is discovered via DY with a $\sim$100 fb^{-1} or smaller data set, one can still eliminate the possibility of fake bZ' signals from ccZ' coupling by combining bZ' and cZ' searches. For instance, a 600 GeV Z' with $g_{cc}^R = 0.02$, which can be discovered with 110 fb^{-1} of data via the DY process, requires 1310 fb^{-1} of data to give fake bZ' signals at 5σ; however, observing cZ' does not take long after the discovery of the DY process (e.g., 160 fb^{-1} for Conf2 and 350 fb^{-1} for ctagT; see the left panel of Fig. 1, Fig. 2, and the right panel of Fig. 4). In general, fake bZ' signals from ccZ' coupling, if observed, should be preceded by the discovery of cZ' with a smaller data set. A similar argument holds for fake cZ' from bbZ' coupling: after discovery via DY induced by bbZ', fake cZ' can emerge, but it should be preceded by the discovery of bZ' for all five c-tagging schemes (see the right panels of Figs. 1 and 3, and the left panel of Fig. 4). Therefore, the simultaneous search for cZ' and bZ' can reveal if the coupling behind DY production is ccZ' or bbZ'.

V. PRESENCE OF BOTH cZ' AND bZ' PROCESSES

We have so far studied the discovery potential of cZ' and bZ' processes with a nonzero ccZ' or bbZ' coupling exclusively. However, all uuZ', ddZ', ssZ', ccZ', and bbZ' couplings could in principle coexist. If any of the first three couplings involving light quarks are nonzero, we might discover Z' in the DY process, without the subsequent discovery of cZ' and/or bZ' processes which can be easily discerned by using both c- and b-tagging algorithms.

A more interesting scenario is when both ccZ' and bbZ' couplings are nonzero, but all other couplings to light quarks

TABLE IV. Signal and background cross sections (in fb) after selection cuts for a 150 GeV Z' (with $g_{bb}^R = 0.005$) via $pp \to bZ' + X \to b\mu^+\mu^- + X$ (plus the conjugate process) at the 14 TeV LHC.

Signal	$Z/\gamma^* + b$ jet	$Z/\gamma^* + c$ jet	Z/γ^*+ light jet	$t\bar{t}$	Wt	VV	$t\bar{t}V$	tWZ	Total Bkg.
1.31	11.35	6.89	2.53	53.21	4.28	2.69	0.05	0.01	81.01

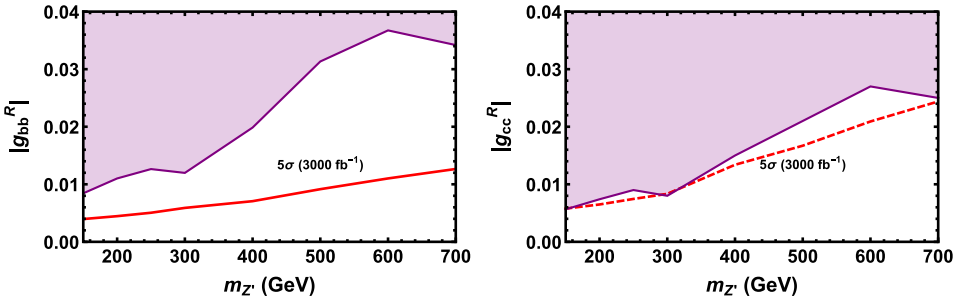

FIG. 4. Discovery reach of bZ' originating from g_{bb}^R (left) and g_{cc}^R (right) couplings at the 14 TeV LHC with 3000 fb^{-1} of data.

vanish. These couplings would give rise to both cZ' and bZ' processes, depending on their individual strengths. In order to investigate such a scenario, we take the following benchmark point:

$$m_{Z'} = 150 \text{ GeV}, \qquad g_{cc}^R = 0.003, \qquad g_{bb}^R = 0.005.$$

These g_{cc}^R and g_{bb}^R values remain within their respective allowed regions, and $\sigma(pp \to Z' + X) \cdot \mathcal{B}(Z' \to \mu^+\mu^-)$ remains within the 95% CL upper limit set by ATLAS [1]. Larger g_{cc}^R and g_{bb}^R would be in tension with the $\sigma \cdot \mathcal{B}$ upper limit.

This benchmark can be discovered in the DY process with just 210 fb^{-1} integrated luminosity, followed by a discovery in the bZ' process with 870 fb^{-1} of data, which is lower than that quoted for the case with only $g_{bb}^R = 0.005$ in Sec. IV A. The cZ' process would emerge later, at 2370 (Conf1), 2420 (Conf2), 2570 (ctagL), 2600 (ctagM), or 1740 fb^{-1} (ctagT). The benchmark thus illustrates the possibility of uncovering both charm and bottom couplings of a new Z' resonance, and the efficacy of the HL-LHC. Further sharpening of heavy-flavor tagging tools would be helpful.

VI. SUMMARY

We analyzed the possibility to probe the coupling structure of a relatively weakly coupled Z' via the $qg \to qZ'$ process, adopting c- and b-tagging algorithms from ATLAS and CMS at the 14 TeV LHC. Such a resonance would appear first in the Drell-Yan process. Our study showed that, if a Z' is discovered first via the $pp \to Z' + X \to \mu^+\mu^- + X$ DY production, one could then discover $cg \to cZ'$ and $bg \to bZ'$ processes at the HL-LHC. We illustrated this using two different c-tagging schemes from ATLAS, which were chosen to optimally reduce $Z+$ light-jet background but maintain moderate c-tagging efficiencies. We also adopted three c-tagging working points from CMS in our analysis.

The cZ' process could arise from the misidentification of light or b jets. Fake cZ' from light-jet misidentification can be excluded by existing data, if one adopts the ATLAS Conf2 or CMS ctagT scheme. However, none of the c-tagging schemes can rule out the possibility of fake cZ' from the mistagging of b jets. In order to eliminate fake cZ' from finite bbZ' coupling, we advocate the simultaneous study of cZ' and bZ' processes. We found that a nonzero bbZ' coupling would give genuine bZ' and fake cZ' signatures. Conversely, a nonzero ccZ' coupling can give genuine cZ' and fake bZ' signatures, within the allowed region of ccZ' coupling. The latter possibility can be eliminated in the near future if no Z' emerges in the DY process with ~250 fb^{-1} of data. Our study is based on the current status of c-tagging algorithms. Any future improvement in c tagging would only improve the analysis.

It would be interesting if both ccZ' and bbZ' couplings are nonzero. We illustrated this with one such representative scenario, i.e., for a 150 GeV Z' with $g_{cc}^R = 0.003$ and $g_{bb}^R = 0.005$. We found that 210 fb^{-1} of data is needed for DY discovery, which would be followed by the discovery of the bZ' process with 870 fb^{-1}, while the cZ' process would emerge much later with integrated luminosities ranging from ~1740 to 2600 fb^{-1}, depending on the c-tagging scheme. This scenario differs from cases when either g_{cc}^R or g_{bb}^R vanish. For example, when only $g_{cc}^R = 0.005$ is nonzero, DY discovery for a 150 GeV Z' would be followed by discovery in the cZ' process, without the emergence of a subsequent 5σ signature of the fake bZ' process, even with full HL-LHC data. However, if $g_{bb}^R = 0.005$ is the only nonzero coupling, the DY process would be followed by discovering the bZ' process. The highest attainable fake cZ' signature in this scenario would be about 4.4σ.

We have not included backgrounds associated with fake and nonprompt sources, systematic uncertainties, and QCD corrections for the signal, which would induce some uncertainties in our results. Furthermore, we have not included the uncertainties from scale dependence and PDFs, with the latter being large for the heavy quarks, in particular for the b quark. The PDF uncertainties for c- or b-quark-initiated processes were discussed in Refs. [36,37], while a detailed discussion on PDF choices and their uncertainties for Run 2 of the LHC can be found in Ref. [38]. All of these effects would have an impact on the extracted upper limits on the g_{cc}^R and g_{bb}^R couplings, as well as our estimated luminosities for discovery.

Our study illustrates that new resonances could still emerge at the LHC, and large integrated luminosities can probe weaker couplings or reveal more details. Given that our study was partly motivated by flavor "anomalies" [39–42], the associated flavor of Z' production could shed

more light on potential new physics indications from the flavor sector. Of course, one would certainly search for other Z' decay modes, such as $Z' \to \tau^+\tau^-$ implied by Eq. (1).

ACKNOWLEDGMENTS

This work is supported by Grants No. NTU-ERP-106R8811 and No. NTU-ERP-106R104022, and MOST 105-2112-M-002-018, 106-2811-M-002-187 and 106-2112-M-002-015-MY3. W. S. H. thanks G. N. Taylor for hospitality.

Note added.—While revising the manuscript, we noticed that CMS released a new result [43] for the dilepton resonance search with 36 fb^{-1} of data from the 13 TeV LHC. We checked the resulting 95% CL upper limits on different g^R_{qq} couplings, with the procedure to interpret the CMS results discussed in Ref. [3], and found that the new CMS limits [43] are comparable to the ATLAS limits with 36 fb^{-1} of data [1], except for $m_{Z'} \sim 500$ GeV, where CMS gives slightly stronger limits due to a sharp downward fluctuation in its observed data. We confirmed that the new CMS limits do not have an impact on our conclusion.

APPENDIX A: SIGNAL AND BACKGROUND FOR THE DY PROCESS

The dominant backgrounds associated with DY production are the Z/γ^* and $t\bar{t}$ processes, with subdominant contributions from Wt, VV, $t\bar{t}V$, and tWZ productions, where $V = W$, Z. Selected events should contain two oppositely charged muons with transverse momenta $p_T^\mu > 50$ GeV, and an invariant-mass cut of $|m_{\mu\mu} - m_{Z'}| < 15$ GeV is imposed. Signal and background processes are generated at LO via MadGraph5_aMC, interfaced to PYTHIA 6.4 and fed into the fast detector simulator DELPHES 3.4.0, following the MLM prescription for the ME and PS matching and merging. The QCD correction factors for the $t\bar{t}$, Wt, and VV backgrounds are the same as those described in Sec. III. However, the Z/γ^* cross section is corrected up to NNLO QCD + NLO EW by a factor of 1.27, obtained by FEWZ 3.1 [44]. The impact of the selection cuts on different backgrounds are given in Table V for various Z' masses. Note that, just like cZ' and bZ' processes, we do not include a K factor for the signal.

TABLE V. Background cross sections (in fb) for the DY process after selection cuts, for various $m_{Z'}$ values.

$m_{Z'}$ (GeV)	150	200	300	400	500	600	700
Total Bkg.	2327	842	177	55	20	9	5

APPENDIX B: KINEMATIC DISTRIBUTIONS

Normalized kinematic distributions for the cZ' process ($m_{Z'} = 150$ GeV) and its backgrounds are shown in

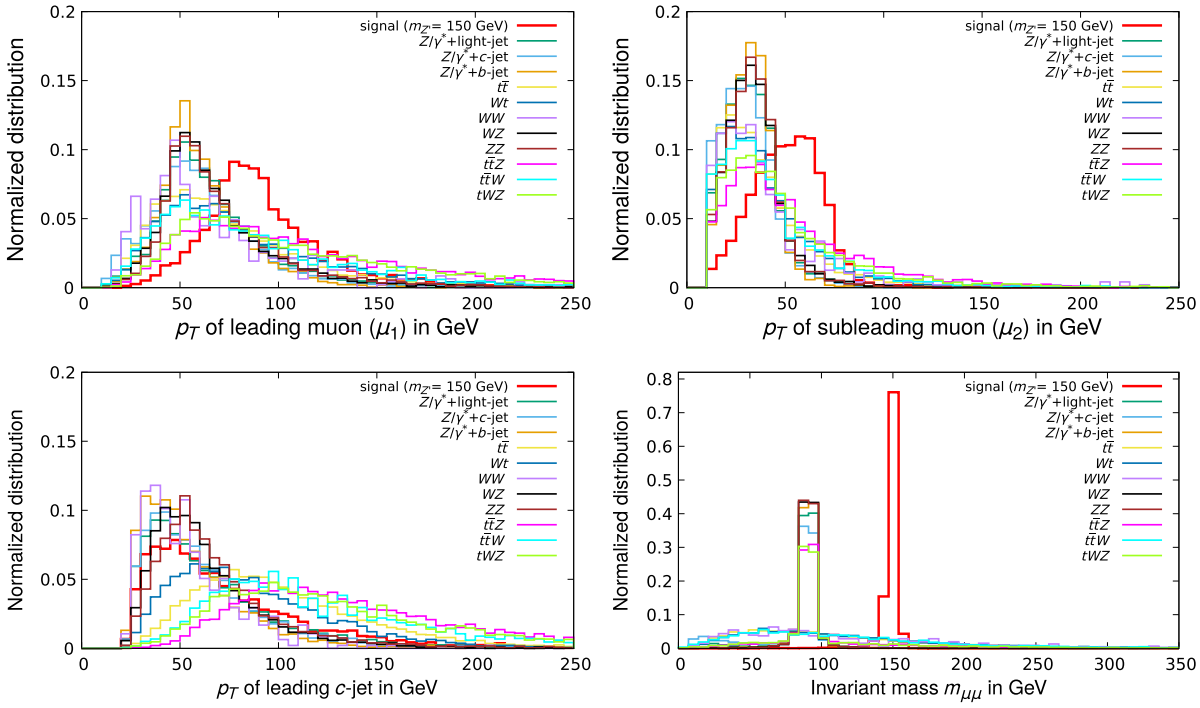

FIG. 5. Normalized distributions of various kinematic variables for the cZ' process ($m_{Z'} = 150$ GeV) and its backgrounds: transverse momenta of the leading muon (upper left), subleading muon (upper right), and leading c jet (lower left), and the dimuon invariant mass (lower right). See text for details.

Fig. 5. Specifically, they are generated with default cuts of MADGRAPH5_AMC for $g^R_{cc} = 0.005$ and ctagT, but other choices for g^R_{cc} and the c-tagging scheme should give the same normalized distributions. The latter is in part because we assume constant c-tagging efficiencies with respect to p_T and η of the jet, but recovering mild dependencies on them would not affect the normalized distributions significantly.

[1] M. Aaboud *et al.* (ATLAS Collaboration), J. High Energy Phys. 10 (2017) 182. The $\sigma(pp \to Z' + X) \cdot \mathcal{B}(Z' \to \mu^+\mu^-)$ 95% CL upper limit is available, along with other auxiliaries, at https://atlas.web.cern.ch/Atlas/GROUPS/PHYSICS/PAPERS/EXOT-2016-05/.

[2] CMS Collaboration, Report No. CMS-PAS-EXO-16-031.

[3] W.-S. Hou, M. Kohda, and T. Modak, Phys. Rev. D **96**, 015037 (2017).

[4] ATLAS Collaboration, Report No. ATL-PHYS-PUB-2015-001.

[5] ATLAS Collaboration, Report No. ATL-PHYS-PUB-2017-013.

[6] CMS Collaboration, Report No. CMS-PAS-BTV-16-001.

[7] G. Aad *et al.* (ATLAS Collaboration), J. Instrum. **11**, P04008 (2016).

[8] CMS Collaboration, Report No. CMS-PAS-BTV-15-001.

[9] K. Fuyuto, W.-S. Hou, and M. Kohda, Phys. Rev. D **93**, 054021 (2016).

[10] X. G. He, G. C. Joshi, H. Lew, and R. R. Volkas, Phys. Rev. D **43**, R22 (1991).

[11] R. Foot, Mod. Phys. Lett. A **06**, 527 (1991).

[12] W. Altmannshofer, S. Gori, M. Pospelov, and I. Yavin, Phys. Rev. D **89**, 095033 (2014).

[13] J. Alwall, R. Frederix, S. Frixione, V. Hirschi, F. Maltoni, O. Mattelaer, H.-S. Shao, T. Stelzer, P. Torrielli, and M. Zaro, J. High Energy Phys. 07 (2014) 079.

[14] R. D. Ball, V. Bertone, S. Carrazza, L. D. Debbio, S. Forte, A. Guffanti, N. P. Hartland, and J. Rojo (NNPDF Collaboration), Nucl. Phys. **B877**, 290 (2013).

[15] T. Sjöstrand, S. Mrenna, and P. Z. Skands, J. High Energy Phys. 05 (2006) 026.

[16] J. Alwall *et al.*, Eur. Phys. J. C **53**, 473 (2008).

[17] C. Delaunay, T. Golling, G. Perez, and Y. Soreq, Phys. Rev. D **89**, 033014 (2014).

[18] G. Perez, Y. Soreq, E. Stamou, and K. Tobioka, Phys. Rev. D **92**, 033016 (2015); **93**, 013001(E) (2016).

[19] I. Brivio, F. Goertz, and G. Isidori, Phys. Rev. Lett. **115**, 211801 (2015).

[20] G. W. -S. Hou (ATLAS and CMS Collaborations), Proc. Sci. CHARM2016 (**2016**) 088.

[21] S. Iwamoto, G. Lee, Y. Shadmi, and Y. Weiss, J. High Energy Phys. 09 (2017) 114.

[22] T. Han and X. Wang, J. High Energy Phys. 10 (2017) 036.

[23] T. Cohen, M. Freytsis, and B. Ostdiek, J. High Energy Phys. 02 (2018) 034.

[24] U. Haisch, arXiv:1706.09730.

[25] A. M. Sirunyan *et al.* (CMS Collaboration), Eur. Phys. J. C **78**, 287 (2018).

[26] J. de Favereau, C. Delaere, P. Demin, A. Giammanco, V. Lemaître, A. Mertens, and M. Selvaggi (DELPHES 3 Collaboration), J. High Energy Phys. 02 (2014) 057.

[27] R. Boughezal, X. Liu, and F. Petriello, Phys. Rev. D **94**, 074015 (2016).

[28] ATLAS and CMS recommended predictions for top-quark-pair cross sections can be found at, https://twiki.cern.ch/twiki/bin/view/LHCPhysics/TtbarNNLO.

[29] N. Kidonakis, Phys. Rev. D **82**, 054018 (2010).

[30] T. Gehrmann, M. Grazzini, S. Kallweit, P. Maierhöfer, A. von Manteuffel, S. Pozzorini, D. Rathlev, and L. Tancredi, Phys. Rev. Lett. **113**, 212001 (2014).

[31] M. Grazzini, S. Kallweit, D. Rathlev, and M. Wiesemann, Phys. Lett. B **761**, 179 (2016).

[32] F. Cascioli, T. Gehrmann, M. Grazzini, S. Kallweit, P. Maierhöfer, A. von Manteuffel, S. Pozzorini, D. Rathlev, L. Tancredi, and E. Weihs, Phys. Lett. B **735**, 311 (2014).

[33] J. Campbell, R. K. Ellis, and R. Röntsch, Phys. Rev. D **87**, 114006 (2013).

[34] J. M. Campbell and R. K. Ellis, J. High Energy Phys. 07 (2012) 052.

[35] ATLAS Collaboration, Report No. ATLAS-CONF-2014-058.

[36] M. Buza, Y. Matiounine, J. Smith, and W. L. van Neerven, Eur. Phys. J. C **1**, 301 (1998).

[37] F. Maltoni, G. Ridolfi, and M. Ubiali, J. High Energy Phys. 07 (2012) 022; 04 (2013) 95.

[38] J. Butterworth *et al.*, J. Phys. G **43**, 023001 (2016).

[39] R. Aaij *et al.* (LHCb Collaboration), Phys. Rev. Lett. **111**, 191801 (2013).

[40] R. Aaij *et al.* (LHCb Collaboration), Phys. Rev. Lett. **113**, 151601 (2014).

[41] R. Aaij *et al.* (LHCb Collaboration), J. High Energy Phys. 02 (2016) 104.

[42] R. Aaij *et al.* (LHCb Collaboration), J. High Energy Phys. 08 (2017) 055.

[43] A. M. Sirunyan *et al.* (CMS Collaboration), arXiv:1803.06292.

[44] Y. Li and F. Petriello, Phys. Rev. D **86**, 094034 (2012).